

## Chapter 2. Development of Fast-Slow Coincidence Setup with $\text{LaBr}_3(\text{Ce})$ Detectors

PAC measurements, as already discussed, are of two types depending on the resolving time of the coincidence circuitry, interaction time and the lifetime of the intermediate state of the probe nucleus. If the resolving time of the set-up is less than the lifetime of intermediate level, one goes for time differential measurements. On the other hand, if the resolving time is larger compared to the intermediate level then one has to go for time integral measurements.

In TDPAC measurements a time spectrum is obtained by the coincidence counting of two photons in a cascade as a function of the time difference between the two photons. The PAC experiments are carried out using a fast-slow coincidence setup. The role of fast coincidence part is to establish the time relationship between two photons and the slow part is to discriminate the  $\gamma$ -energies. The TDPAC spectrometer should fulfil some criteria, viz., the detectors should be able to detect all the  $\gamma$ -quanta with maximum efficiency in order to enhance statistics of the coincidence measurements, solid angle per detector should be as small as possible in order to prevent the loss of the angular part of the perturbation function, the energy resolution of the detectors should be sufficient to distinguish between two cascading  $\gamma$ -rays of interest and separate them from other irrelevant  $\gamma$ -rays, if any and time resolution of the setup should be as good as possible, preferably better than 1ns.

The coincidence setup used in the present thesis is based on CAMAC. Computer Automated Measurement And Control (CAMAC) is a standard bus for Data acquisition and control. The bus allows data exchange between plug-in modules (up to 24 in a single crate) and a crate controller, which then interfaces to PC. Within the dataway, modules are addressed by slot (Geographical addressing). The left-most 22 slots are available for application modules while the right-most two slots are dedicated to a crate controller. The CAMAC based setup acquires all the coincidence

data in LIST mode and the gates are given between the relevant  $\gamma$ -energies in the post-acquisition period. So, data for more than one probe can be extracted in a single experiment and the gates can be given in the post-acquisition period among the different  $\gamma$ -cascades relevant to the respective probes in order to extract the informations for different probes separately in a single measurement. For this, the detectors should be able to distinguish all the  $\gamma$ -cascades involved in the probes used and the lifetime of the intermediate states for the different probes should be comparable so that the gated coincidence spectra for all the different probes can be adjusted in the same time-scale.

The circuit diagram of the Fast-Slow coincidence setup is shown in Fig. 2.1:

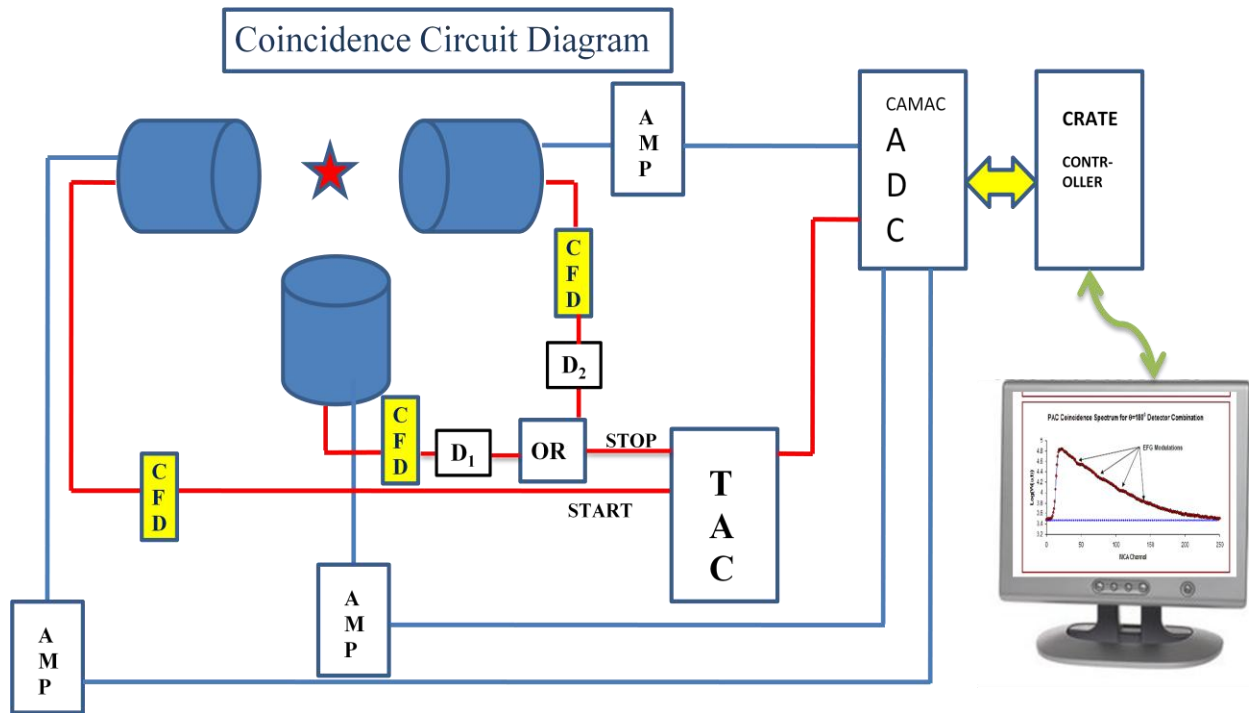


**Figure 2.1:** Fast-Slow coincidence circuit diagram for TDPAC measurement.

The circuit has several components and each of these components will be discussed one by one in the context of their role in the coincidence measurement. The basic components of TDPAC

system are three detectors each coupled to PM tube. There are two outputs from each PM tube, viz., Dynode output and Anode output. Dynode output is used for energy discrimination while the anode output is used for timing measurements. Three dynode outputs are fed into three amplifier (AMP) model no: Ortec 572 and the amplified outputs are fed into the CAMAC Quad Analogue to Digital Converter (ADC) model no: AD413A. Negative anode output from the photomultiplier tube is taken through a constant fraction discriminator (CFD) model no: Ortec 584 which produces a fast logic pulse by taking the rise part of the input pulse. The time spectrum is obtained by using a time-to-amplitude converter (TAC) model no: Ortec 467. One CFD output which detects first  $\gamma$ -photon of the cascade acts as a START signal to TAC and either of the two CFD outputs detecting second  $\gamma$ -photon of the cascade at  $90^\circ$  and  $180^\circ$  acts as a STOP signal to TAC. The two STOP signals from CFDs are delayed ( $D_1$  for  $90^\circ$  detector and  $D_2$  for  $180^\circ$  detector generally with  $D_2 > D_1$ ) and passed through logic OR gate when the logic output acts as the STOP signal to TAC. This is the timing or the fast part of coincidence circuit. This gives the coincidence with respect to time only. TAC will generate a pulse, the height of which is proportional to the time difference between the two events. The data acquisition was performed with LAMPS software [185]. The Single Channel Analyzer (SCA) output of TAC is used as the master gate to ADC.

The spectrometer consists of three planar  $\text{LaBr}_3(\text{Ce})$  detectors and source is kept at a distance of 1-2 cm. from the detector. The activity of the source is generally kept to be  $\sim 30\text{-}40$  KHz to get a coincidence count rate of  $\sim 1\text{-}2$  kbps. The unipolar output from each of the amplifiers with a shaping time of  $1\ \mu\text{s}$  is used for the energy measurement. The gain of the amplifiers is so adjusted that the  $\gamma$ -ray of interest lies in the middle of the 8K channel. The added advantage of the present coincidence setup is that if there is any sudden drift in the amplifier during acquisition, the

energy-gates can be accordingly adjusted in the post-acquisition period. The time walk for each of the three CFDs is adjusted from the monitor output triggered by the CFD output. The threshold adjustment for each CFD is performed depending on the energy of the  $\gamma$ -ray and the bias voltage applied to the corresponding PM tube. However, in the present work all the measurement has been performed at a negative bias of 2500V. The threshold is so adjusted that the chance coincidences are minimized without hampering the true coincidence. The delay in each of the CFD has been adjusted in such a way that the two coincidence spectra at  $90^\circ$  and  $180^\circ$  are well separated with respect to the life time of the intermediate level of the probe atom. The TAC output is checked for it to fall within the mastergate provided by its SCA output. The time calibration for the TAC is performed by Ortec time calibrator model 462 in order to adjust the time per channel (TPC) depending on the lifetime of the intermediate level. The CAMAC ADC output is connected to PC by a CAMAC Crate Controller CMC100. Before each acquisition, the time resolution of the system is checked with a prompt source.

### **2.1. Detectors:**

The nature and the size of the detector are important to decide the time resolution of the circuit. The detector should have fast timing characteristics for the scintillation, i.e., the rise time of the output light should be as small as possible. In this regard, plastic scintillators [186] are well known. But the plastic scintillators have very low efficiency and poor energy resolution.

In the present measurement,  $\text{LaBr}_3$  (Ce) scintillator detectors with an improved energy resolution were used in the present work. BrillanCe<sup>TM</sup>380 [ $\text{LaBr}_3$  (Ce)] [187] is a transparent scintillator material that offers the best energy resolution, fast emission and excellent linearity. It has a higher light output than  $\text{NaI(Tl)}$  and also better energy resolution. In the present thesis, 30mmX30mm  $\text{LaBr}_3$  (Ce) detectors have been used with energy resolution of  $\sim 3\%$  at 662keV

energy. An improved energy resolution has been achieved with this detector due to its high scintillation output of  $\sim 63$  photons/keV [188], compared to other available scintillators. A low decay time of  $\sim 20$  ns makes it ideal for timing measurements from few ns to few picoseconds.

For a particular detector, its size is of significant importance in deciding its time response. Larger the size of the crystal, greater is the variation in the path length of the photons, generated at different points of the crystal, in reaching the photocathode. Consequently, the distribution in the time of arrival of the photons at the photocathode increases resulting in the increase in the width of the time response function. Therefore, a smaller crystal will give a better time response, but the efficiency decreases with smaller volume. So a compromise is made between the size of the crystal and its efficiency to optimize the time response function. A large volume detector with a very high efficiency cannot be used in a timing measurement.

## **2.2. Photo Multiplier Tube:**

The detector is coupled to PM Tube and the PM Tube has a very important role in deciding the time response function. The spread in the transit time of the photoelectrons through the dynodes of the PM tube contributes to the spread in the distribution of the time response. The transit time in a PM tube is defined as the average time difference between the arrival of the photon at photocathode and collection of the subsequent electron burst at the anode. The spread in the transit time arises due to the difference in the path lengths of the electrons generated at different parts of photocathode and also between the dynodes. Further, the distribution in the initial velocities of the photoelectrons leaving the photocathode also results in the spread in the transit time. If the initial velocity is less, there will be large variation of transit time for the electrons having different path lengths. However if the velocity is large, this spread in transient time is reduced for the same path length distribution. So it is desirable to have higher initial velocity for

the photoelectrons to get a sharper time response. This is done by using larger voltage difference between the photocathode and the first dynode. Other factors related to PM tubes that affect the time resolution are;

- (i) Number of dynodes in the PM tube has significant role in the response function. Fewer stages of multiplication give better timing since this reduces the spread in the transit time of electrons.
- (ii) Smaller is the diameter of the photocathode, better is the time resolution. If the diameter of the photocathode is smaller the distribution of path length between the photocathode and dynode reduces. So the transit time reduces. Best timing will be achieved when the central area of the photocathode is illuminated.
- (iii) The design of both K-d1 (cathode to first dynode) region and the electron multiplier are critical in obtaining optimum time performance. The equalisation of the path length to d1 independent of the point of origin should be maintained. The focussing of electron trajectories onto small area of each dynode and short inter-electrode distance reduces this dispersion. This can be achieved by using planoconcave window linear focussed electron multipliers.

Another important property that a PM tube should have is the high gain so that the preamplifier or the amplifier can be avoided and the anode output can be used directly for timing purpose. This would reduce the unnecessary jitter due to extra electronic components. Further, in the use of negative high voltage in the cathode and anode in the ground potential, dc coupled output can be derived from the anode. This procedure reduces the noise level in the output.

In the present thesis, XP2020/URQ fast PM Tube has been used. The XP2020/URQ is a widely used UV sensitive ultra-fast photomultiplier tube with a high gain and short transit time. This

photomultiplier is a focused tube with twelve dynode stages having the highest gain of  $\sim 10^8$ . The tube has a transit time spread down to 0.2 ns and a rise time of 1.4 ns making it suitable to couple to a fast scintillator. Two outputs are furnished: the negative signal from the anode is intended for timing applications and the linear signal from tenth dynode is for energy measurements. The negative high voltage is applied to the cathode and the anode is operated essentially at ground potential. This facilitates the incorporation of several features that augment the fast timing performance. The anode output is dc-coupled with the anode being connected to ground through a 50- $\Omega$  load resistor. This eliminates the base-line shift caused by varying counting rates in ac-coupled systems. It also suppresses reflections by providing back-termination for the anode output connection. The LaBr<sub>3</sub> (Ce) crystals of size 30 mm X 30 mm, sealed inside Al-housing, has been coupled to XP2020/URQ PMT via UV sensitive coupling glue. The energy and timing properties of the detector have been studied at different bias voltages of the tube. The measurements have been performed at different bias voltages of the PMT from 2000 – 2500 V at an interval of 100 V. The energy spectra obtained with the LaBr<sub>3</sub> (Ce) detector, for different sources, are shown in Fig. 2.2.

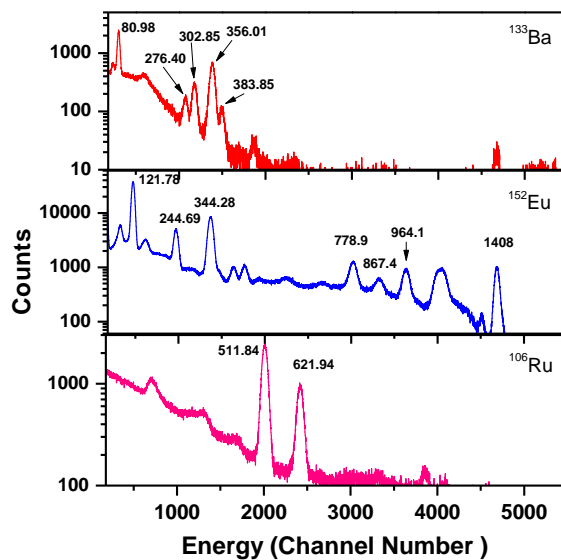


**Figure 2.2:** The energy spectra obtained with LaBr<sub>3</sub> (Ce) detector <sup>133</sup>Ba, <sup>152</sup>Eu and <sup>106</sup>Ru.

The excellent energy resolution of LaBr<sub>3</sub> (Ce) detector can easily be realized from the above figure. The energy response of the detector has been found to be linear up to 622 keV for all the bias voltages. The energy response becomes nonlinear at energies higher than 622 keV for all the bias voltages above 2000 Volt as shown in Fig. 2.3. The energy resolutions have been determined from the Full Width at Half Maxima (FWHM) of the obtained photo peaks. The study shows that the energy resolution of the detector does not change much with the variation of bias voltages. However, at almost all the bias voltages the energy resolution at 622 keV comes around 3% which is comparable to the best resolution obtained for this detector.

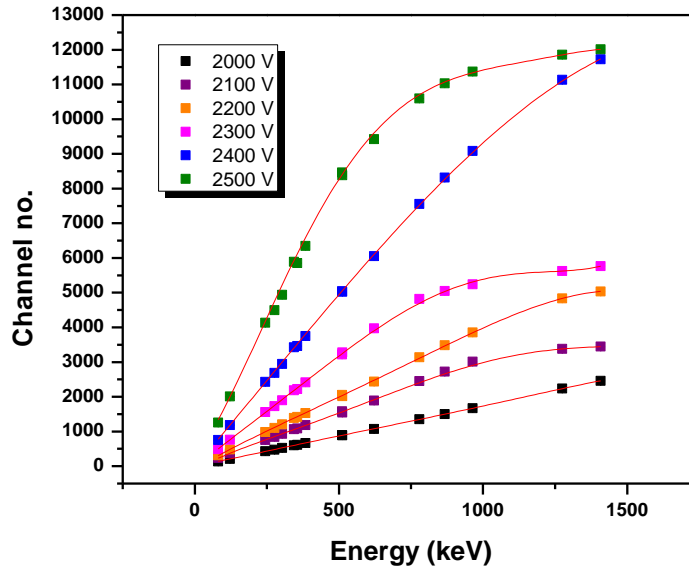


**Figure 2.3:** The energy response curve for LaBr<sub>3</sub> (Ce) detector up to 1.4 MeV.

This information on the energy linearity of LaBr<sub>3</sub> (Ce) detector has an important application in the extraction of data during post-acquisition period by putting gates between different  $\gamma$ -cascades, specially while working with multi-probe systems as mentioned earlier.

### 2.3. Resolving Time:

For a fast-slow coincidence setup, the resolving time of the fast-slow coincidence unit is the measure of the width of the time distribution of the coincidence counts of two simultaneous

events. In principle, the coincidence counts should show a single line for simultaneous events. However due to the variation in the response of the detectors for different events, photomultiplier tubes and the electronic modules, a distribution develops in the time response resulting in the widening of the line spectrum. Amplitude and time walk in the time pick-off lead to a finite resolving time of the coincidence circuit. Prompt time spectrum has been measured for the 511-511 keV cascade for the  $^{22}\text{Na}$  positron annihilation and shown in Fig. 2.4. The time resolution is  $340 \pm 10$  ps with the  $\text{LaBr}_3(\text{Ce})$  detector.

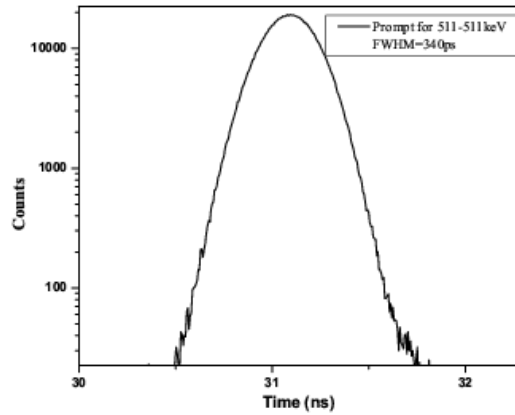


**Figure 2.4:** Prompt for 511-511 cascade of  $^{22}\text{Na}$  source.

The FWHM of the TAC peaks has been estimated at different bias voltages in order to study the time resolution of the  $\text{LaBr}_3(\text{Ce})$  detector coupled to the same XP2020/URQ PMT. The best time resolution is obtained at 2500 Volt bias voltage. The variation of time resolution with bias voltage of the PM Tube has been shown in Fig. 2.5 up to 2400 Volt.

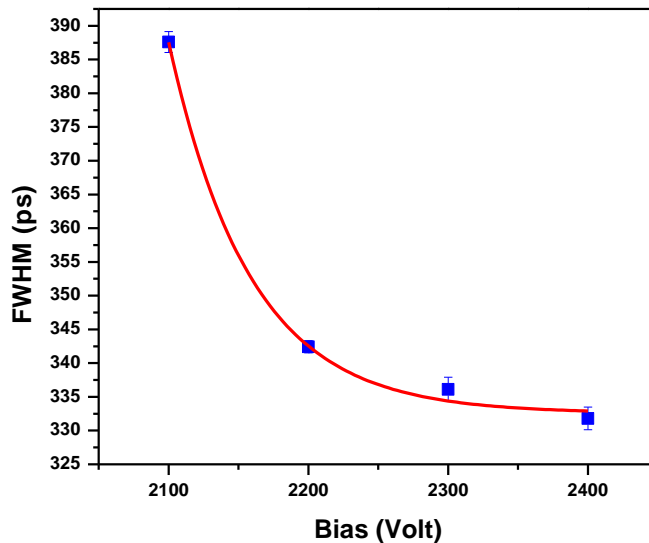


**Figure 2.5:** The variation of time resolution of the detector at different bias voltages.

The variation of time resolution with the high voltage can be explained in terms of the transit time of electrons from photocathode to anode.

#### 2.4. Electronic Modules:

The **amplifier** is one of the most important components in a pulse-processing system for applications in counting, timing or energy spectroscopy. The simplest concept for pulse shaping is the use of a CR high-pass filter followed by an RC low-pass filter. This pulse-shaping technique can be used with scintillation detectors. For that application, the shaping time constant should be chosen to be at least three times the decay time constant of the scintillator to ensure complete integration of the scintillator signal. The disadvantage of using the CR-RC shaping with scintillation detectors is the much longer pulse duration compared with that of single-delay-line shaping. In the present case, the dynode pulse from PM tube is fed into the amplifier and amplifier output is directly fed into the ADC to get the energy spectrum. The shaping time

constant of the amplifier has been set to  $1\mu\text{s}$  and the gain has been adjusted according to the energy of the cascade  $\gamma$ -rays used in different measurements.

**Fast timing discriminators** are designed to achieve the best time resolution and the highest counting rates by operating on the fast-rising detector signal. The negative anode pulse from the PM tube is directly fed into the fast timing discriminator. The “rise time” refers to the time taken to make the transition from 10% to 90% of the pulse amplitude on the leading edge of the pulse. The primary function of a timing discriminator is to mark the arrival time of the detected events with precision and consistency. The timing discriminator has to be chosen in a proper way based on the characteristics of the detector and intended application in order to get the optimum time resolution. Jitter, walk and drift are the three major factors limiting time resolution. Walk can be of two types: time walk and amplitude walk. Time jitter and time walk apply to cases where the amplitudes of the input pulses are constant. The effect due to amplitude walk is realized when the amplitudes of the input pulses are varying. An important source of time jitter is the random fluctuation in the size and shape of the signal pulse. Such fluctuations appear due to the electronic noise added by the components which process the linear pulses prior to the time pick-off. Other sources of jitter are of discrete nature of the electronic signal as generated in the detector. When the number of information carriers that make up the signal is less, statistical fluctuation and time of occurrence of the ion pairs is reflected in the size and shape of the pulse. This effect is large for small pulses and for detectors that generate less number of information carriers. Drift is the long term error introduced by the component aging and by temperature variation during long measurement periods.

In the time pickoff process, two ways of triggering are possible to derive the logic time signal from an analog input, viz., leading edge triggering and constant fraction triggering. A leading-

edge triggering incorporates a simple voltage comparator with its threshold set to a desired voltage. “Walk” is normally the dominant limitation on time resolution with this method. Again, the contribution from time jitter is associated with scintillation detector due to the statistical fluctuations in the arrival time of the pulse at the detector output. The existence of an optimum triggering fraction in leading-edge timing with scintillation detectors stimulated the design of a circuit that would always trigger at the optimum fraction of the pulse height for any pulse height [189-190]. This is known as Constant Fraction Discriminator (CFD). The additional benefit of CFD is the elimination of amplitude walk. Here, the input signal is split into two parts: one fraction is attenuated to a fraction ‘ $f$ ’ of the original amplitude and the other part is delayed and inverted. These two signals are subsequently added to form the constant-fraction timing signal which is a bipolar signal with a zero-crossing time. Since the time of zero-crossing is independent of pulse-amplitude, the CFD delivers virtually a zero walk at the expense of jitter. Walk and jitter are minimized by the proper adjustment of the zero-crossing reference and by selection of the correct attenuation factor and delay. Again time jitter can be reduced by reducing the number of electronic components. One obvious way of doing this is to take the dc coupled anode output from the PM tube where the additional capacitor circuit between anode and CFD can be avoided. Another important modification is to use high gain PM tube so that the amplification of the anode output from the PM tube is not required. The timing resolution from a CFD is better than that from leading-edge timing. With scintillation type of detectors, a fraction somewhere between 0.2 and 0.4 is a reasonable choice.

When a timing application demands picoseconds precision, a **Time to Amplitude Converter** (TAC) is the right solution. TAC converts the time interval between “start” and “stop” signals into voltage. The output of a TAC is a rectangular pulse with a width of a few microseconds and

amplitude that is proportional to the time interval between “start” and “stop” pulses. Typically, the fast CFD outputs are used as the start and stop signals to TAC. By adding a single-channel pulse-height analyzer (SCA) to the output of a TAC, it can be used to identify the coincidence events between two detectors. The SCA output from the TAC acts as the “master gate” to ADC, i.e., only those TAC pulses which fall within the SCA window will be analyzed by the ADC. The SCA threshold can be adjusted to ensure that only the events in the peak are accepted. Subsequently, the SCA output can be used as the coincidence gate when analyzing the energy spectrum from scintillation detector on the ADC. TAC is used for the measurements on time ranges less than 10  $\mu\text{s}$  when time resolution from 10 ps to 50 ns is required. TAC range is adjusted according to the resolution required for that particular measurement. In a  $\gamma\text{-}\gamma$  coincidence measurement, the lifetime of the intermediate level decides the TAC resolution required for that measurement. Another parameter called as Time Per Channel (TPC) is defined for a particular coincidence measurement. For that, time calibration of TAC is performed by inserting cable delays of known length between the timing discriminator output and TAC input. For higher accuracy in time-calibration, a separate time-calibrator can be a better choice. It uses an accurate digital clock to produce stop pulses at precisely spaced intervals after a start pulse.

An **Analogue to Digital Converter** (ADC) measures the maximum amplitude of an analogue pulse and converts that value to a digital number. This digital output is a proportional representation of the analogue amplitude at the ADC input. For sequential arriving of pulses, a histogram is generated representing the spectrum of the input pulse heights. There are two types of ADC, viz., Wilkinson ADC and successive-approximation ADC. In the present work CAMAC 8K ADC which is of second type has been used.

## 2.5. Energy of Photons:

The width of the instrumental response, apart from being dependent on the aforesaid factors, depends strongly on the energy of the photon. The energy of the photons decides the number of information carriers that make up the signal. As the photon energy reduces, the height of the anode pulse reduces and consequently the slope of the leading edge of the pulse is also reduced. So the time uncertainty due to jitter increases and so does the response function.

## 2.6. Data Reduction:

A least-square fitting of the experimental coincidence data with the theoretical expression for the perturbation function, modified with the effect of asymmetry of EFG, frequency distribution and resolving time of the coincidence circuit, using a software Winfit version 3.0.4 [191]. The fitting program extracts the TDPAC parameters, viz.  $\omega_Q, \eta, \delta$ , with errors. The software also carries out cosine type fast fourier transform to find out all the interaction frequencies with their individual populations. From the measured data, the true coincidences are obtained by subtracting background, accidental coincidences and contributions from other coincident  $\gamma$ -rays present in the source. The true number of coincidences can now be written as:

$$C^t(\vartheta) = Mp_1p_2\Omega_1\varepsilon_1\Omega_2\varepsilon_2\varepsilon_cK(\vartheta) \quad (1.105)$$

M is the number of nuclear disintegration per unit time,  $p_i$  the probability per disintegration that the radiation selected in counter  $i$  is emitted,  $\Omega_i$  the solid angle in unit of  $4\pi$ ,  $\varepsilon_i$  the efficiency of channel  $i$  and  $\varepsilon_c$  the efficiency of the coincidence circuit.  $K(\vartheta)$  denotes the directional correlational function as measured with the instrument.

The  $\chi^2$  value indicates a first clue to the fit performance. This value should be as small as possible and in the ideal case close to one. The program is iteration-based meaning that it changes the initial parameters until  $\chi^2$  becomes minimized. In this fitting process, spectra can be

added, inverted or even the theoretical function can be subtracted from the data to visualize potential modulations in the residual spectra. So, all the fractions, present in the sample, can be seen individually. The cross correlation analysis [192] is helpful in choosing good start values for the fit. It can also serve to get an idea of frequency distributions. Suppose we have a single fraction and the two parameters  $V_{zz}$  and the asymmetry parameter. Instead of plotting these two parameters, it is more convenient to plot  $V_{xx}$  versus  $V_{yy}$  or even better to plot  $Y = -2V_{xx}$  versus a linear combination of  $V_{xx}$  and  $V_{zz}$ , i.e.,  $X = 2(2V_{zz} + V_{xx})/\sqrt{3}$ . This is exactly what the Czjzek-plot does. Alternatively, the abscissa and the ordinate can also be expressed in terms of  $\omega_Q(\sqrt{3} + \eta/\sqrt{3})$  and  $\omega_Q(1 - \eta)$ .

Lastly, it is to be kept in mind that the coincidence rate  $K(\vartheta)$  corresponds to the correlation function only under the assumption of centered point sources and point detectors. In order to compare the experimental results with theoretical calculations, the coefficients  $A_{kk}^{exp}$  must be corrected for the deviations from an ideal arrangement. First, it has to be corrected for the finite solid angle of the counters and secondly, the corrections for the finite source extension while working with large sources (e.g., axial source) are also necessary. After having corrected the coefficients  $A_{kk}$  for finite solid angle and finite source extension, one is left with the problem of correcting them for in the source. There are two effects: (i) some of the  $\gamma$ -rays get deflected before being counted. This effect, caused by Compton scattering, tends to smear out the correlation by decreasing the magnitude of the coefficients. (ii) The  $\gamma$ -ray pairs that give coincidences in the  $90^\circ$  direction are on the average less absorbed than those pairs giving coincidences in the  $180^\circ$  direction. Thus one misses more coincidences at  $\theta = 180^\circ$  than at  $\theta = 90^\circ$ . The absorption is very pronounced for low  $\gamma$ -ray energy and sources with high atomic number  $Z$ . If the radioactive source is very thin but surrounded by scattering material,

then only effect (i) is present and correlation is attenuated. The corrections due to scattering in the source are treated in ref. [193].

## **2.7. Conclusion:**

A new methodology of coincidence counting using CAMAC electronics and LaBr<sub>3</sub>(Ce) detectors has been introduced. The present TDPAC spectrometer with LaBr<sub>3</sub>(Ce) detector system has the best energy resolution and reasonable time resolution. It has been demonstrated that the present fast-slow coincidence setup has got several advantages due to the incorporation of LaBr<sub>3</sub>(Ce) detectors and the CAMAC data-acquisition system. Again, the interplay of all the electronic components is also significant for the setup. The energy linearity of the new detector system coupled to fast PM tubes has been studied and the dependence of time resolution of the coincidence circuit has been presented. The behaviour of the detector with other fast PM tube can also be studied in order to optimize the utility of the LaBr<sub>3</sub>(Ce) detector system. The PAC probes having close  $\gamma$ - $\gamma$  cascade can be studied with this new system. The energy gates can be precisely selected due to an excellent energy resolution of the LaBr<sub>3</sub>(Ce) detectors and the systems containing more than one probe can be studied in a single experiment. The present setup can be applied in the measurement of nuclear level lifetime of  $\sim$ ps order due to its excellent time resolution. Hence, the scope of this new TDPAC spectrometer is highly widened both in the field of material science and nuclear spectroscopy.